nature geoscience

LETTERS

PUBLISHED ONLINE: 26 APRIL 2009 | DOI: 10.1038/NGEO503

Eocene Tibetan plateau remnants preserved in the northwest Himalaya

Peter van der Beek[1]*, Jérémie Van Melle[1], Stéphane Guillot[1], Arnaud Pêcher[1], Peter W. Reiners[2], Stefan Nicolescu[2] and Mohammad Latif[3]

The northwest Himalaya shows strongly contrasting relief. Deeply incised mountain ranges that are characterized by extremely rapid exhumation[1–3] and some of the highest peaks in the world are in contrast with high-elevation, low-relief areas such as the Deosai plateau in northern Pakistan, which lies at an altitude of 4,000 m. The origin and evolution of such plateau regions at the convergence of the most active continental collision in the world remain elusive. Here we report low-temperature thermochronology data from the Deosai plateau and use thermal history modelling to show that the plateau has undergone continuous slow denudation at rates below 250 m Myr^{-1} for the past 35 Myr at least. This finding suggests tectonic and morphologic stability of the plateau since at least Eocene times, only 15–20 Myr after the onset of the India–Asia collision. Our work contradicts the hypothesis that widespread low-relief surfaces in the northwest Himalaya result from efficient kilometre-scale glacial erosion during Quaternary times[4]. We show that similarly stable surfaces exist throughout the entire northwest Himalaya and share common morphologic characteristics and denudation histories, which are comparable to those of the western Tibetan plateau. Our results suggest that these surfaces are preserved remnants of an Eocene southwestern Tibetan plateau that was more extensive than today.

The Himalayan syntaxes have attracted much attention over the past decade because they appear as areas in which potential coupling between tectonics and surface processes can be demonstrated (see, for example, refs 2, 5). In the northwest Himalaya (Fig. 1), studies have mainly focused on the very rapidly exhuming Nanga Parbat massif [2,3,5] and, to a lesser extent, the Karakorum mountains[6,7]. However, the northwest Himalayan syntaxis also contains widespread low-relief regions that are characterized by much slower exhumation rates[8] and that have received much less attention.

The observed morphological variations correlate with major geologic units in the northwest Himalaya. High-elevation, low-relief regions are mainly found within the Kohistan–Ladakh arc complex; the backbone of the northwest Himalaya that separates the Indian and Asian plates. The Karakorum range to the north constitutes the former Eurasian margin that collided with the Kohistan–Ladakh arc along the Shyok suture zone after ~75 Myr (ref. 9 and references therein). The Kohistan–Ladakh arc was in its turn thrust over Himalayan rocks of the Indian plate along the Indus–Tsangpo suture zone after the onset of Himalayan collision at ~55 Myr (refs 10–12). Major crustal thickening, high-grade metamorphism and building of topography occurred between ~55 and 40 Myr (ref. 13), followed by rapid exhumation of the Nanga Parbat antiform since Late Miocene time[3].

We use morphologic analyses to identify high-elevation low-relief surfaces throughout the northwest Himalaya and western Tibetan plateau (Fig. 1), defining them as broad (at least several tens of km^2) regions with elevations over 3,800 m and topographic slopes less than 17° (excluding modern glacier surfaces; see Fig. 1, caption). The widespread Tibetan plateau surface is clearly mapped out by this approach, rising from ~4,900 m in the Lhasa terrain south of ~33° N to ~5,500 m in the Qiantang and Kunlun terrains to the north.

The Karakorum fault is generally regarded as the western border of the Tibetan plateau (see, for example, refs 9, 14). However, our morphologic analysis identifies several prominent plateau areas to the southwest of this boundary. From east to west, these are the Zada basin in southwest Tibet, Tso Morari in northwest India and the Deosai plateau in northern Pakistan. Although the former constitutes a Neogene internally drained basin that was only recently captured by the Sutlej River[15], both Tso Morari and Deosai clearly represent externally drained low-relief erosional surfaces. Moreover, both the Kohistan region to the west of Nanga Parbat, and the Ladakh batholith to the east of Deosai, contain widespread summit regions with low slopes (Fig. 1). A topographic swath profile from Kohistan to southwest Tibet, across Nanga Parbat, Deosai and the Ladakh batholith, highlights remarkable continuity in the plateaux and low-slope summit regions, which rise gently from ~4,000 m in the west to ~5,000 m in Tibet.

The relief characteristics of the Deosai plateau and surrounding regions are further illustrated in Fig. 2. The mean and modal elevations of the Deosai plateau and Kohistan are similar to that of the intervening Nanga Parbat massif (Fig. 2a), lending support to the hypothesis that uplift and exhumation in the latter is fundamentally driven by localized incision of the Indus River[2,5]. The modal elevations of the Karakorum range and Ladakh batholith are significantly higher (~4,700 m) than those of the regions to the west. In contrast, the frequency distributions of normalized elevations (Fig. 2c, d) indicate a strong morphologic contrast between Kohistan, Deosai and the Ladakh batholith on the one hand, and Nanga Parbat and the Karakorum on the other: the former show negatively skewed elevation distributions and high hypsometric integrals (~0.7), whereas the latter are characterized by much more symmetric distributions of topography (hypsometric integrals of 0.5 and 0.58, respectively).

Slope distributions as a function of elevation (Fig. 2b) show that the modal elevation peaks in Kohistan and Deosai correspond to low-slope regions. In a previous morphometric study of the region[4], it was suggested that such high-elevation low-relief areas resulted from efficient glacial erosion during Quaternary times, independent of morphology or exhumation rate. However, the slope minima are

[1]LGCA-OSUG, University of Grenoble, CNRS, BP 53, F-38041 Grenoble, France, [2]Department of Geosciences, University of Arizona, Tucson, Arizona 85721, USA, [3] Geological Survey of Pakistan, Plot N.84, H-8/1 Islamabad, Pakistan. *e-mail: pvdbeek@ujf-grenoble.fr.

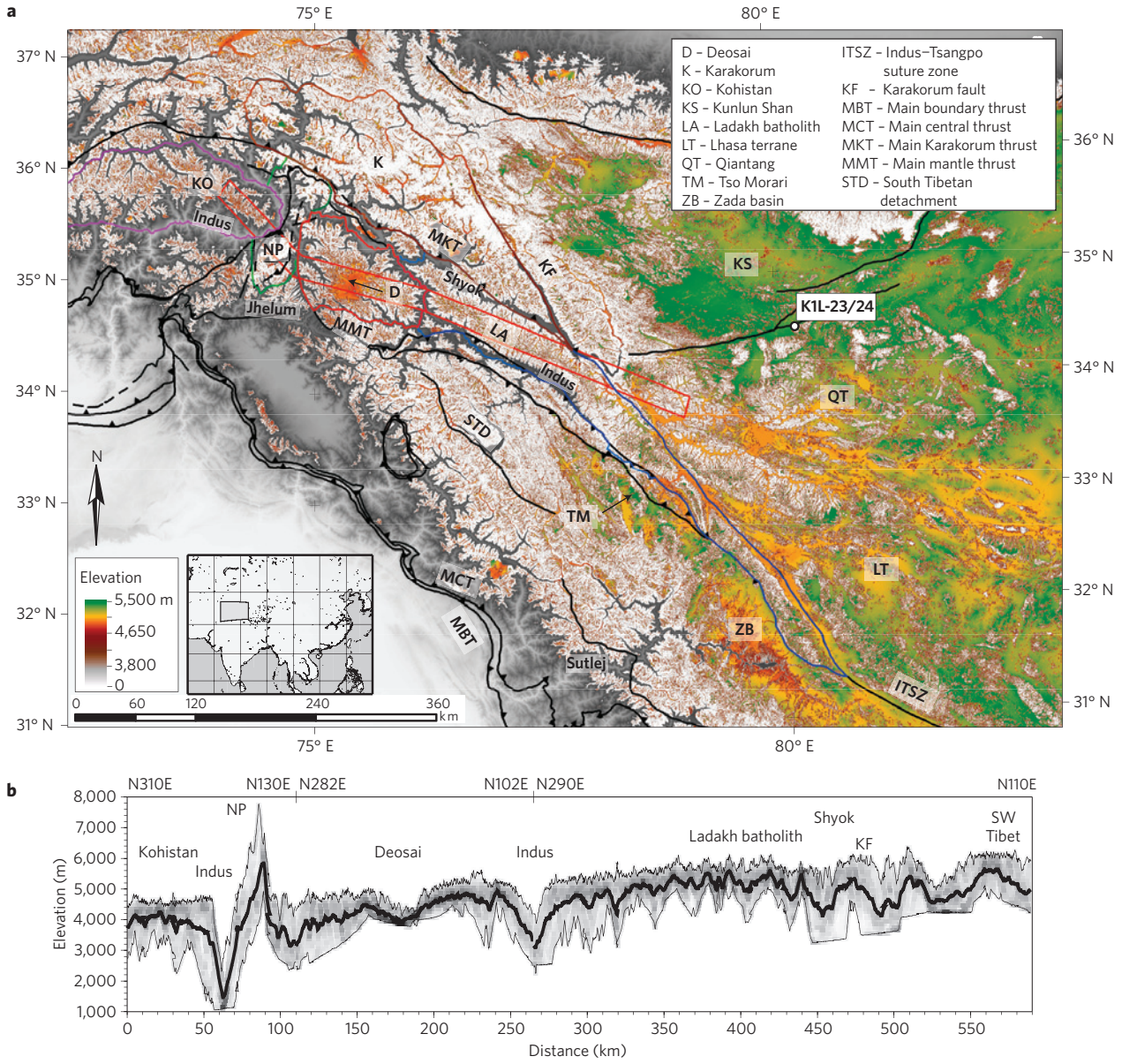

Figure 1 | Topography and relief characteristics of the northwest Himalaya and western Tibet. a, Map showing high-elevation low-relief regions (coloured according to elevation) and major tectonic elements. High-elevation low-relief regions are defined as those with elevation greater than 3,800 m and slope less than 17°. Elevations lower than 3,800 m are shown in grey scale; regions above 3,800 m with slopes greater than 17° are in white. Ice- and snow-covered regions are also in white; these were identified using their spectral characteristics on Landsat7 ETM+ imagery and extracted to exclude smooth high-elevation glacier surfaces in the Karakorum. Note that some highly perched flat valley bottoms and debris-covered glaciers remain, in particular in the Karakorum mountains and western Tibet. Coloured outlines delineate regions for which morphological characteristics are shown in Fig. 2; the red box shows the location of the topographic swath profile shown in **b**. The location of sample K1L23/24 from western Tibet is also shown. Geographic regions mentioned in the text and main tectonic elements are indicated (key in legend), as well as main south-draining river systems (Indus, Shyok, Jhelum and Sutlej). The inset shows the location within Asia. **b**, A longitudinal (west-northwest/east-southeast) topographic swath profile from Kohistan to southwest Tibet, crossing the Nanga Parbat massif (NP), Deosai plateau and Ladakh batholith. The profile shows mean (thick line), maximum and minimum (thin lines) elevations, as well as the probability density of the elevation along the swath (grey scale from 0—white—to 0.5—black).

much more prominent in Kohistan, Deosai and, to a lesser extent, the Ladakh batholith than in the Nanga Parbat and Karakorum massifs, highlighting the geomorphic difference between the high- and lower-relief regions.

To elucidate the denudation history of the Deosai plateau, we report apatite fission-track (AFT) and apatite and zircon (U–Th)/He (AHe, ZHe) thermochronology data in Fig. 3 and Supplementary Tables S1–S4. These three thermochronometers record cooling below closure temperatures of 110 ± 10, 70 ± 10 and 180 ± 20 °C, respectively[16,17]. Samples were collected at elevations between 2,500 and 4,000 m on the plateau surface, as well as on its northeast rim and in the high Astor valley, which drains the plateau to the west. AFT ages vary between 14.6 ± 1.1 and 27.0 ± 3.5 Myr, with the youngest ages encountered in the Astor valley and the oldest on the northeast plateau rim. For the higher-closure-temperature ZHe system, weighted mean ages from replicate determinations vary between 22.1 ± 1.0 Myr for a sample collected at 2,960 m elevation on the northeast flank of the plateau and 39.4 ± 7.4 Myr for the central plateau (3,960 m elevation). The lower-temperature AHe ages are consistent with the other

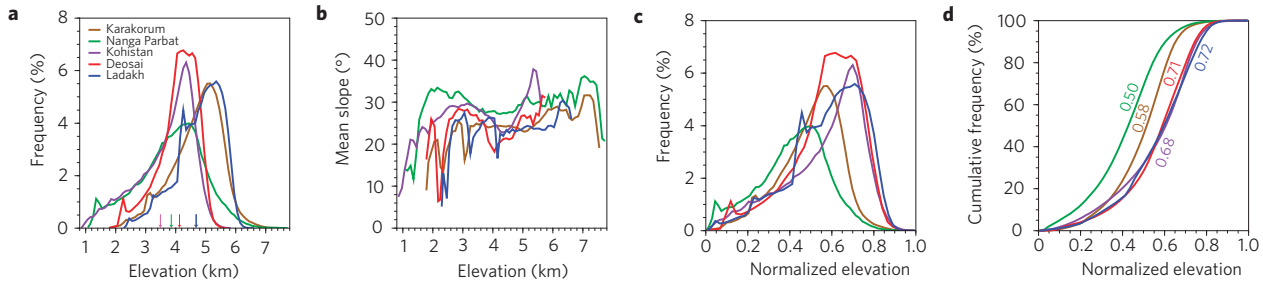

Figure 2 | Morphometry of the Deosai plateau and surrounding regions (outlined in Fig. 1). a, Frequency distributions of elevation (binned at 100 m intervals); small arrows indicate mean elevations (Kohistan, 3,490 m; Nanga Parbat, 3,850 m; Deosai, 4,120 m; Karakorum, 4,680 m; Ladakh batholith, 4,690 m). **b**, Mean slope as a function of elevation (binned at 100 m intervals; note that standard deviations of slope values within each bin are of the order of 10°). **c**, Frequency distributions of normalized elevation h', defined as $h' = (h - h_{min})/(h_{max} - h_{min})$, where h_{max} and h_{min} are the maximum and minimum elevations within the region, respectively. **d**, Cumulative frequency distributions of normalized elevation or hypsometric curves. Hypsometric integrals are indicated for the different regions. Note that ice- and snow-covered surfaces were excluded from this analysis.

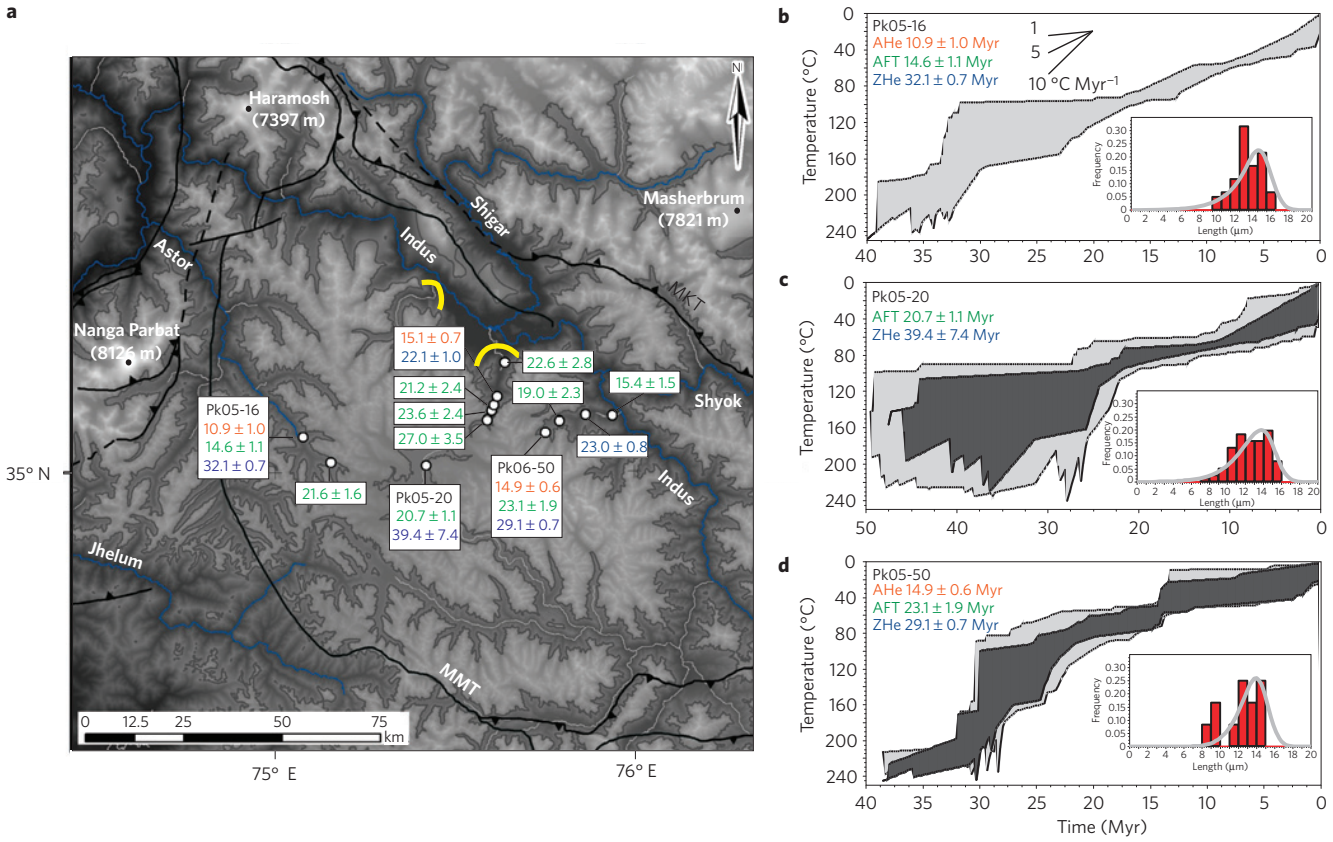

Figure 3 | Low-temperature thermochronology data from the Deosai plateau. a, AHe (orange), AFT (green) and ZHe (blue) ages (in Myr, see Supplementary Tables S2–S4), overlain on a grey-scale elevation map of the plateau. Samples used for thermal history modelling are indicated by their codes. Major tectonic boundaries (black; key as in Fig. 1), rivers (blue), terminal moraines (yellow, after ref. 19) and peaks are also indicated. **b**–**d**, Modelled time–temperature paths for samples from the Deosai plateau. Light-shaded regions encompass thermal histories with an acceptable fit to the data (goodness-of-fit parameter > 0.05); dark-shaded regions encompass thermal histories with a good fit to the data (goodness-of-fit parameter > 0.5; ref. 18). Data constraints on thermal-history inversion (AHe and ZHe ages, AFT ages) are given at the top left of panels; observed (histogram) and predicted (probability curve) fission-track length distributions are shown at the bottom right.

data and vary between 10.9 ± 1.0 Myr in the Astor valley and 15.1 ± 0.3 Myr on the eastern rim. Overall, these ages imply cooling and exhumation rates that are one to two orders of magnitude lower than those encountered in the adjoining Nanga Parbat and Karakorum massifs[2,3,6].

We have modelled the cooling histories of three samples from the plateau surface, for which we have thermochronology data for multiple systems, using a thermal history inversion model[18] that takes into account AFT ages, track-length distributions and kinetic parameters as well as AHe and ZHe ages. The model can infer thermal histories from the AFT data alone but the AHe and ZHe data enable better constraint of the low-temperature part of the history and extrapolation to higher temperatures, respectively. The envelopes of cooling histories that fit the data are all consistent with constant slow cooling at rates of ~5 °C Myr^{-1} since at least 35–40 Myr ago (Fig. 3), implying constant long-term denudation rates not exceeding 125–250 m Myr^{-1} since this time for reasonable values (20–40 °C km^{-1}) of the geothermal gradient.

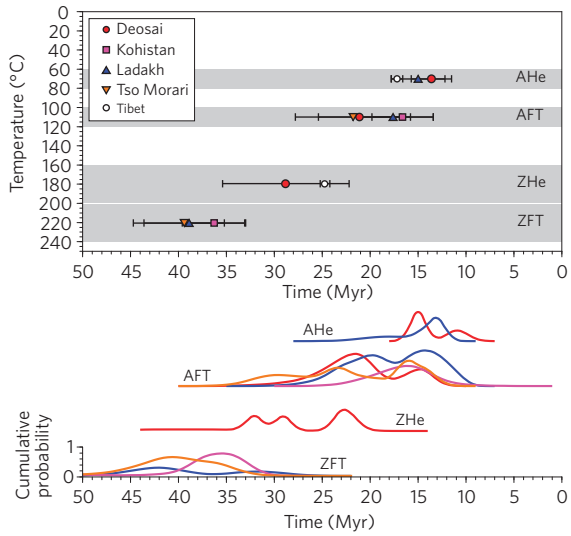

Figure 4 | Comparison of thermochronological ages from high-elevation low-relief regions in the northwest Himalaya. Data are from the Deosai plateau surface (this study), elevations greater than 3,000 m in western Kohistan (ref. 8), elevations greater than 4,000 m in the Ladakh batholith (refs 23, 24) and elevations greater than 4,600 m in Tso Morari (ref. 25). The upper panel shows the mean age and standard deviation of each dataset plotted against closure temperature for each thermochronometer (ranges indicated by shaded boxes). Also plotted are single AHe and ZHe ages (1σ errors) from sample K1L-23/24 from Longmu-Co, Western Tibet (this study). The lower plot shows cumulative probability-density functions of thermochronometer ages for these datasets, using the same colour coding.

The inferred history of constant slow denudation of the plateau has several major implications: first, it contradicts the hypothesis that widespread low-relief surfaces in the northwest Himalaya result from efficient, kilometre-scale glacial erosion during Quaternary times[4]. Although the Deosai plateau was repeatedly glaciated during the Quaternary[19,20], it has not suffered significantly increased glacial erosion rates, which would have been recorded as a phase of rapid recent denudation that is not observed in the data. Denudation of the Deosai plateau has clearly not equilibrated to base-level lowering imposed by the Indus River, which incises at rates at least an order of magnitude higher[1,21], supporting the idea that low-relief surfaces in the northwest Himalaya represent relict landscapes (see, for example, ref. 20 and references therein).

Second, continuous slow denudation since Eocene times, that is, only 15–20 Myr after the onset of India–Asia collision, implies that the Deosai plateau developed early in the Himalayan history and limits the phase of orogenic relief growth in the Ladakh–Kohistan arc to the early Paleogene. Although thermochronology data do not directly record surface uplift, the simplest explanation for the inferred constant denudation rates is that the plateau had already reached its present-day elevation during the Eocene. Early uplift of the Kohistan–Ladakh arc, with respect to the Himalayan core, is supported by the volcanic–sedimentary source signature of early Paleogene foreland-basin deposits in Pakistan and northwest India (ref. 22 and references therein).

When comparing our inferred cooling history for the Deosai plateau with scattered thermochronology data from the other plateaus and low-slope summit regions in the northwest Himalaya, a surprisingly consistent picture appears (Fig. 4). AFT ages from elevations greater than 3,000 m in western Kohistan are 15–19 Myr (ref. 8), whereas zircon fission-track (ZFT) ages determined on the same samples and recording cooling from 220 ± 20 °C (refs 16, 17) are 34–38 Myr. In the Ladakh batholith, samples from elevations greater than 4,000 m are characterized by AFT ages between 15 and 25 Myr (refs 23, 24), with age–elevation relationships indicating apparent exhumation rates of ~100 m Myr^{-1} between ~30 and ~10 Myr (ref. 23). Two ZFT ages from the Ladakh batholith are 41–43 Myr (ref. 23). Samples from the high-elevation Tso Morari surface[25] yield AFT ages between 15 and 30 Myr and ZFT ages of 35–45 Myr; these data were interpreted as recording rapid exhumation between 50 and 40 Myr ago, followed by steady and slow denudation rates since that time[11,25].

It thus seems that all high-elevation, low-relief areas in the northwest Himalaya show coincident histories of slow continuous cooling since the Middle Eocene. No published thermochronology data are available from western Tibet with which to compare these histories, but we have analysed a sample from our collection (see Fig. 1 for location) that yielded an AHe age of 17.2 ± 0.6 Myr and a ZHe age of 24.7 ± 0.5 Myr, suggesting similar cooling histories (Fig. 4). The comparable cooling histories and morphological continuity of the western Tibetan plateau and the high-elevation low-relief surfaces in the northwest Himalaya support a common origin.

The uplift history of the Tibetan plateau constitutes one of the main controversies of the past two decades in the earth sciences; recent data concur to support pre/mid-Tertiary uplift of its southern and central parts (the Lhasa and Qiantang terrains)[14,26–28]. Our analysis supports this scenario and moreover suggests that the surface remnants we recognize in the northwest Himalaya formed part of an elevated and more extensive Tibetan plateau in Eocene times. Importantly, the recognized plateau remnants occur both north (Deosai, Kohistan, Ladakh) and south (Tso Morari) of the Indus–Tsangpo suture zone, thus sealing it. This pleads for a rapid and short initial orogenic phase in the northwest Himalaya, during which crustal thickening led to building of significant topography between 55 and 40 Myr ago (refs 12, 13).

Dismemberment of this southwesternmost part of the Eocene Tibetan plateau may date from the Early Miocene, when deformation and uplift of the Himalayan orogenic wedge and backthrusting along the Indus suture zone led to the development of longitudinal drainage of the Indus River[29] and incision of the former plateau area. Simultaneously or slightly later, onset of motion along the Karakorum fault[30] also guided drainage into the southwestern Tibetan plateau and led to the development of its present-day western margin. The long-term preservation of plateau remnants within this very dynamic setting implies that the base-level change due to incision of major rivers since Early Miocene times has not yet propagated fully into the landscape.

Methods

Apatite and zircon were extracted from rock samples using standard magnetic and heavy-liquid techniques. For AFT analysis, apatites were mounted in epoxy, polished and etched in a 5.5 M HNO_3 solution at 20 °C for 20 s. All samples were dated by the external detector method, using U-poor mica as external detector and a zeta calibration factor for Fish Canyon and Durango age standards. Samples were irradiated at the well-thermalized ORPHEE facility of the *Centre d'Etudes Nucléaires* in Saclay, France, with a nominal fluence of ~5×10^{15} neutrons cm^{-2}. Neutron fluences were monitored using IRMM540 and NBS962 dosimeter glasses. Mica detectors were etched in 48% HF at 20 °C for 18 min. All samples were analysed by J. Van Melle. In samples that were selected for thermal-history modelling, confined track-length measurements were performed by digitizing the track ends using a drawing tube; the etch-pit width parallel to the C axis (D_{par}) of 100 tracks crossing the etched internal surface was measured using the same digitizing technique.

(U–Th)/He thermochronometry was performed at the University of Arizona. Preparation included selection of grains for euhedral shape, appropriate size and, in the case of apatite, absence of inclusions. Single-crystal aliquots of apatite and zircon were wrapped in Nb foils and degassed by laser heating. He abundances were measured using ^{3}He isotope dilution and quadrupole mass spectrometry. Degassed aliquots were dissolved and U and Th concentrations were measured by isotope dilution using an ELEMENT 2 sector inductively coupled plasma–mass spectrometer. An α-ejection correction was applied to derive the corrected (U–Th)/He age, following ref. 31.

Thermal-history modelling was performed using HeFTy v1.3 software[18]. Input data for the inversions included AFT, AHe and ZHe ages, grain size, the AFT track-length distribution (uncorrected for angle to the *C* axis) and D_{par} values calibrated to the values of standard samples used for deriving the annealing model. Annealing–diffusion algorithms used are those from ref. 32 for apatite fission-track annealing, ref. 33 for AHe diffusion and ref. 34 for ZHe diffusion (see ref. 18 for details). Models were constrained by the present-day surface temperature and boxes placed around the thermochronological ages, with box sizes of 5–15 Myr and 60–100 °C so as not to guide thermal histories (see Fig. 3). Random subsegment spacing was used and no continuous cooling constraint was applied. Models were run until 25 'good' or 200 'acceptable' fits were obtained, as defined in ref. 18.

Received 12 February 2009; accepted 26 March 2009; published online 26 April 2009

References

1. Burbank, D. W. *et al.* Bedrock incision, rock uplift and threshold hillslopes in the northwestern Himalayas. *Nature* **379**, 505–510 (1996).
2. Zeitler, P. K. *et al.* Crustal reworking at Nanga Parbat, Pakistan: Metamorphic consequences of thermal–mechanical coupling facilitated by erosion. *Tectonics* **20**, 712–728 (2001).
3. Schneider, D. A., Zeitler, P. K., Kidd, W. S. F. & Edwards, M. A. Geochronologic constraints on the tectonic evolution and exhumation of Nanga Parbat, western Himalaya syntaxis, revisited. *J. Geol.* **109**, 563–584 (2001).
4. Brozoviç, N., Burbank, D. W. & Meigs, A. J. Climatic limits on landscape development in the northwestern Himalaya. *Science* **276**, 571–574 (1997).
5. Zeitler, P. K. *et al.* Erosion, Himalayan geodynamics, and the geomorphology of metamorphism. *GSA Today* **11**, 4–9 (2001).
6. Foster, D. A., Gleadow, A. J. W. & Mortimer, G. Rapid Pliocene exhumation in the Karakoram (Pakistan), revealed by fission-track thermochronology of the K2 gneiss. *Geology* **22**, 19–22 (1994).
7. Mahéo, G., Guillot, S., Blichert-Toft, J., Rolland, Y. & Pêcher, A. A slab breakoff model for the Neogene thermal evolution of South Karakorum and South Tibet. *Earth Planet. Sci. Lett.* **195**, 45–58 (2002).
8. Zeitler, P. K. Cooling history of the NW Himalaya, Pakistan. *Tectonics* **4**, 127–151 (1985).
9. Yin, A. & Harrison, T. M. Geologic Evolution of the Himalayan–Tibetan Orogen. *Annu. Rev. Earth Planet. Sci.* **28**, 211–280 (2000).
10. Garzanti, E., Baud, E. & Mascle, G. Sedimentary record of the northward flight of India and its collision with Eurasia (Ladakh Himalaya, India). *Geodyn. Acta* **1**, 297–312 (1987).
11. de Sigoyer, J. *et al.* Dating the Indian continental subduction and collisional thickening in the northwest Himalaya: Multichronology of the Tso Morari eclogites. *Geology* **28**, 487–490 (2000).
12. Guillot, S. *et al.* Reconstructing the total shortening history of the NW Himalaya. *Geochem. Geophys. Geosyst.* **4**, 1064 (2003).
13. Treloar, P. J., Williams, M. P. & Coward, M. P. Metamorphism and crustal stacking in the North Indian Plate, North Pakistan. *Tectonophysics* **165**, 167–184 (1989).
14. Tapponnier, P. *et al.* Oblique stepwise rise and growth of the Tibet Plateau. *Science* **294**, 1671–1677 (2001).
15. Gansser, A. *Geology of the Himalayas* (Wiley, 1964).
16. Reiners, P. W. & Ehlers, T. A. (eds) *Low-Temperature Thermochronology: Techniques, Interpretations, and Applications* (Mineralogical Society of America/Geochemical Society, 2005).
17. Braun, J., van der Beek, P. & Batt, G. *Quantitative Thermochronology: Numerical Methods for the Interpretation of Thermochronological Data* (Cambridge University Press, 2006).
18. Ketcham, R. A. in *Low-Temperature Thermochronology: Techniques, Interpretations, and Applications* (eds Reiners, P. W. & Ehlers, T. A.) 275–314 (Mineralogical Society of America/Geochemical Society, 2005).
19. Seong, Y. B. *et al.* Quaternary glacial history of the Central Karakoram. *Quat. Sci. Rev.* **26**, 3384–3405 (2007).
20. Shroder, J. F. Jr, Owen, L. & Derbyshire, E. in *Himalaya to the Sea: Geology, Geomorphology and the Quaternary* (ed. Shroder, J. F. Jr) 132–158 (Routledge, 1993).
21. Leland, J., Reid, M. R., Burbank, D. W., Finkel, R. & Caffee, M. Incision and differential bedrock uplift along the Indus River near Nanga Parbat, Pakistan Himalaya, from ^{10}Be and ^{26}Al exposure age dating of bedrock straths. *Earth Planet. Sci. Lett.* **154**, 93–107 (1998).
22. Najman, Y. The detrital record of orogenesis: A review of approaches and techniques used in the Himalayan sedimentary basins. *Earth-Sci. Rev.* **74**, 1–72 (2006).
23. Kumar, R., Lal, N., Singh, S. & Jain, A. K. Cooling and exhumation of the Trans-Himalayan Ladakh batholith as constrained by fission track apatite and zircon ages. *Curr. Sci.* **92**, 490–496 (2007).
24. Kirstein, L. A., Foeken, J. P. T., van der Beek, P. A., Stuart, F. M. & Phillips, R. J. Cenozoic unroofing history of the Ladakh Batholith, western Himalaya, constrained by thermochronology and numerical modeling. *J. Geol. Soc. London* (2009, in the press).
25. Schlup, M., Carter, A., Cosca, M. & Steck, A. Exhumation history of eastern Ladakh revealed by ^{40}Ar/^{39}Ar and fission-track ages: The Indus River—Tso Morari transect, NW Himalaya. *J. Geol. Soc. Lond.* **160**, 385–399 (2003).
26. Rowley, D. B. & Currie, B. S. Palaeo-altimetry of the late Eocene to Miocene Lunpola basin, central Tibet. *Nature* **439**, 677–681 (2006).
27. DeCelles, P. G. *et al.* High and dry in central Tibet during the Late Oligocene. *Earth Planet. Sci. Lett.* **253**, 389–401 (2007).
28. Wang, C. *et al.* Constraints on the early uplift history of the Tibetan Plateau. *Proc. Natl Acad. Sci.* 4987–4992 (2008).
29. Sinclair, H. D. & Jaffey, N. Sedimentology of the Indus Group, Ladakh, northern India: Implications for the timing of initiation of the palaeo-Indus River. *J. Geol. Soc. Lond.* **158**, 151–162 (2001).
30. Valli, F. *et al.* Twenty million years of continuous deformation along the Karakorum fault, western Tibet: A thermochronological analysis. *Tectonics* **26**, TC4004 (2007).
31. Farley, K. A. in *Noble Gases in Geochemistry and Cosmochemistry* (eds Porcelli, D. P., Ballentine, C. J. & Wieler, R.) 819–843 (Mineralogical Society of America/Geochemical Society, 2002).
32. Ketcham, R. A., Donelick, R. A. & Carlson, W. D. Variability of apatite fission-track annealing kinetics: III. Extrapolation to geological time scales. *Am. Mineral.* **84**, 1235–1255 (1999).
33. Farley, K. A. Helium diffusion from apatite: General behavior as illustrated by Durango fluorapatite. *J. Geophys. Res.* **105**, 2903–2914 (2000).
34. Reiners, P. W., Spell, T. L., Nicolescu, S. & Zanetti, K. A. Zircon (U–Th)/He thermochronometry: He diffusion and comparisons with ^{40}Ar/^{39}Ar dating. *Geochim. Cosmochim. Acta* **68**, 1857–1887 (2004).

Acknowledgements

The Geological Survey of Pakistan and the French Embassy in Pakistan provided support during field work. (U–Th)/He thermochronology was supported by the University of Arizona in the framework of the 2007 He-Dating Workshop in Arizona. Partial support for this work was also provided by the French *Agence Nationale de la Recherche*. We thank Andrew Meigs and Albrecht Steck for constructive comments.

Author contributions

P.v.d.B., J.V.M., S.G., A.P., and M.L. conducted fieldwork; J.V.M. processed samples and conducted thermochronological (AFT and (U–Th)/He) and morphometric analyses; P.W.R. and S.N. conducted and supervised (U–Th)/He analyses; P.v.d.B., S.G., A.P. and J.V.M. designed the study and wrote the paper; all authors discussed and commented on the manuscript.

Additional information

Supplementary information accompanies this paper on www.nature.com/naturegeoscience. Reprints and permissions information is available online at http://npg.nature.com/reprintsandpermissions. Correspondence and requests for materials should be addressed to P.v.d.B.